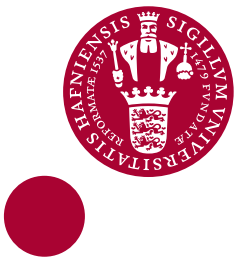

Revisiting the coupling between NDVI trends and cropland changes in the Sahel drylands

a case study in western Niger

Tong, Xiaoye; Brandt, Martin Stefan; Hiernaux, Pierre; Herrmann, Stefanie M.; Tian, Feng; Prishchepov, Alexander; Fensholt, Rasmus

Published in:
Remote Sensing of Environment

DOI:
10.1016/j.rse.2017.01.030

Publication date:
2017

Document version
Peer reviewed version

Revisiting the coupling between NDVI trends and cropland changes in the Sahel drylands: a case study in western Niger

Xiaoye Tong [a], Martin Brandt [a], Pierre Hiernaux [b], Stefanie M. Herrmann [c], Feng Tian [a], Alexander V. Prishchepov [a], Rasmus Fensholt [a]

[a] Department of Geosciences and Natural Resource Management (IGN), University of Copenhagen, 1350 Copenhagen, Denmark

[b] Geosciences Environnement Toulouse (GET), Observatoire Midi-Pyrénées, UMR 5563 (CNRS/UPS/IRD/CNES), 14 Avenue Edouard Belin, 31400 Toulouse, France

[c] School of Natural Resources and the Environment (SNRE), University of Arizona, Office of Arid Land Studies (OALS), 1955 E. Sixth St., Tucson, AZ 85719, USA

Abstract

The impact of human activities via land use/cover changes on NDVI trends is critical for an improved understanding of satellite-observed changes in vegetation productivity in drylands. The dominance of positive NDVI trends in the Sahel, the so-called re-greening, is sometimes interpreted as a combined effect of an increase in rainfall and cropland expansion or agricultural intensification. Yet, the impact of changes in land use has yet to be thoroughly tested and supported by empirical evidence. At present, no studies have considered the importance of the different seasonal NDVI signals of cropped and fallowed fields when interpreting NDVI trends, as both field types are commonly merged into a single 'cropland' class. We make use of the distinctly different phenology of cropped and fallowed fields and use seasonal NDVI curves to separate these two field types. A fuzzy classifier is applied to quantify cropped and fallowed areas in a case study region in the southern Sahel (Fakara, Niger) on a yearly basis between 2000 and 2014. We find that fallowed fields have a consistently higher NDVI than unmanured cropped fields and by using two seasonal NDVI metrics (the amplitude and the decreasing rate) derived from the MODIS time series, a clear separation between classes of fields is achieved (r = 0.77). The fuzzy classifier can compute the percentage of a pixel (250 m) under active cultivation, thereby alleviating the problem of small field sizes in the region. We find a predominant decrease in NDVI over the period of analysis associated with an increased area of cropped fields at the expense of fallowed fields. Our findings couple cropping abandonment (more frequent fallow years) with positive NDVI trends and an increase in the percentage of the cropped area (fallow period shortening) with negative trends. These findings profoundly impact our understanding of greening and browning trends in agrarian Sahelian drylands and in other drylands of developing countries characterized by limited use of fertilizers.

Keywords: NDVI trends, Cropland, Fallowed fields, Phenology, Drylands, Sahel, Niger

1. Introduction

The Sahel is one of the largest dryland regions in the world and is prone to environmental stress and food shortage due to the combined effects of climatic variations and human pressure on land resources. Changes in the human-environmental system of the Sahel became widely apparent in the wake of the severe droughts that occurred in the 1970s and 1980s and one aspect which has received particular attention was the deterioration and loss of the vegetation cover. However, conflicting characterization and interpretation of those changes in vegetation cover are often reported in the scientific literature (Herrmann & Hutchinson, 2005b). This partly stems from incompatible use of research methods and scales of analysis (Rasmussen et al., 2015) and the relative contributions of different climatic and anthropogenic factors to explain those changes are still debated.

Since the early 2000s, several scholars have revealed an ongoing 'greening' of most parts of Sahel from an observed positive trend in time series of the Normalized Difference Vegetation Index (NDVI), interpreted as a proxy of vegetation productivity (Anyamba & Tucker, 2005; Fensholt et al., 2012; Olsson, Eklundh, & Ardö, 2005). Change in precipitation has been identified as the major driver of the observed changes in vegetation greenness (Hickler et al., 2005; Huber, Fensholt, & Rasmussen, 2011; Kaspersen, Fensholt, & Huber, 2011). However, the re-greening is not fully explained by climatic factors, but likely influenced by human management of natural resources, which results in an increase of vegetation productivity (Herrmann, Anyamba, & Tucker, 2005a). For a region particularly reliant on rain-fed agriculture, it is vital to understand the coupling between NDVI trends and vegetation changes in the agrarian Sahel. However, conflicting hypotheses have been reported: on the one hand an expansion (into native savanna) and intensification (fertilizer) of cropland cultivation, and on the other hand agricultural land abandonment, caused by, e.g., the civil war in Sudan (Fuller, 1998; Olsson et al., 2005) may both

contribute to the observed positive trends. Still at present, little scientific empirical evidence for the link between NDVI trends and cropland changes is provided for drylands in general, and for the Sahel region in particular.

Several local scale studies showed a general increase in cropped areas since the 1950s (van Vliet et al., 2013) and in recent years, a few studies have indicated that cropland has a higher annual NDVI than savanna in Sahelian areas, supporting a possible link between cropland expansion/cropping intensification and the observed positive trends in NDVI (Bégué, Vintrou, Ruelland, Claden, & Dessay, 2011; Nutini, Boschetti, Brivio, Bocchi, & Antoninetti, 2013). The linkage between NDVI trends and the role of fallowed fields, as a part of the crop-fallow rotation cycle, should however be taken into account and better studied. In the Sahel, shifting cultivation is the traditional cropping system, by which the fields are cultivated for a given period and then left as fallow for a series of years to restore soil fertility (De Rouw & Rajot, 2004). Fallowed fields are dominated by annual herbaceous plants interspersed with bushes and a sparse tree cover, which is functionally comparable to the vegetation composition of natural savanna. Cropped fields and fallowed fields should have quite different seasonal greenness signals, with the greenness signal of fallowed fields approximating that of savanna. As current classification schemes of the land cover class 'cropland' encompass fallowed fields in both time and space for the Sahel, there is a need to determine the impact of fallow fields on the NDVI signal and related trends.

From the Earth Observation (EO) perspective, a successful differentiation between cropped and fallowed fields is required to improve our understanding of the mechanisms and drivers of observed NDVI trends in relation to changes in the spatio-temporal patterns of crop-fallow rotation due to cropping expansion/abandonment. One of the enduring challenges is the lack of suitable historical Land-Use and Land-Cover Change (LULCC) products documenting the extent of and changes in cropland at the Sahel scale over time (Vintrou et al., 2012). Additionally, fallowed fields have never

been separated from cropland among existing regional and global scale land cover classifications – in higher spatial resolution data such as Landsat (GlobeLand 30) or in relatively low spatial resolution such as SPOT-VGT (e.g., GLC2000: 1 km), MODIS data (e.g., MCD12Q1: 250 m - 1 km) and PROBA-V (100 m) (Lambert, Waldner, & Defourny, 2016). However, cropped and fallowed fields have different growing cycles because of the differences in vegetation composition and influences of human management, such as tillage, weeding, and crop harvesting. Differences in growing cycles, such as emergence, growth, maturity, and harvest/senescence, can potentially help to separate cropped and fallowed fields by extracting the unique vegetation phenological signatures using NDVI derived seasonal metrics (Alcantara, Kuemmerle, Prishchepov, & Radeloff, 2012). This approach has been successfully applied in dryland woody cover monitoring (Brandt et al., 2016) and fodder biomass modeling (Diouf et al., 2015).

The overall objective of our study is thus to develop an improved basis for understanding the role of changes in areas under cultivation on EO vegetation greening trends in the Sahelian drylands. Specifically, we aim to: (1) Analyze intra-annual seasonal NDVI signatures of the cropped and fallowed fields, (2) separate and map cropped and fallowed fields by image classification using satellite-derived seasonal metrics from time series of MODIS NDVI and fuzzy classification techniques to overcome problems of mixed pixels, and (3) link the NDVI trends to the observed changes in cropped and fallowed fields over an observation period spanning from 2000-2014. To do so, detailed spatio-temporal ground-based knowledge is needed; this study makes use of a unique record of field observations of Sahelian crop-fallow rotation in the Fakara region, western Niger (Hiernaux & Turner, 2002).

2. Study area

2.1 Study area in Fakara, Niger

The study area is the district of Dantiandou, located 80 km east of Niamey, the capital city of Niger (Fig. 1). It is situated in the Fakara region, which lies between the Niger River to the west and the Dallol Bosso valley to the south of the line extending from Niamey to Baleyara (Hiernaux & Ayantunde, 2004). Being part of the central Sahel bio-climatic zone (Hiernaux & Ayantunde, 2004), the climate is typical of the semi-arid monsoonal tropics, with an average annual precipitation of about 500 mm but varying spatially and fluctuating from year to year (Barbé & Lebel, 1997). The rural population has increased steadily in the district since the 1950s, leading to an expansion of cultivated areas (Hiernaux et al., 2009). The crop-fallow rotation practiced to manage soil fertility (Turner & Hiernaux, 2015) is typical for the extensive cropping system in the Sahel. Land use/cover has been extensively studied in the district and monitored annually over 20 years (Cappelaere et al., 2009; Hiernaux et al., 2009).

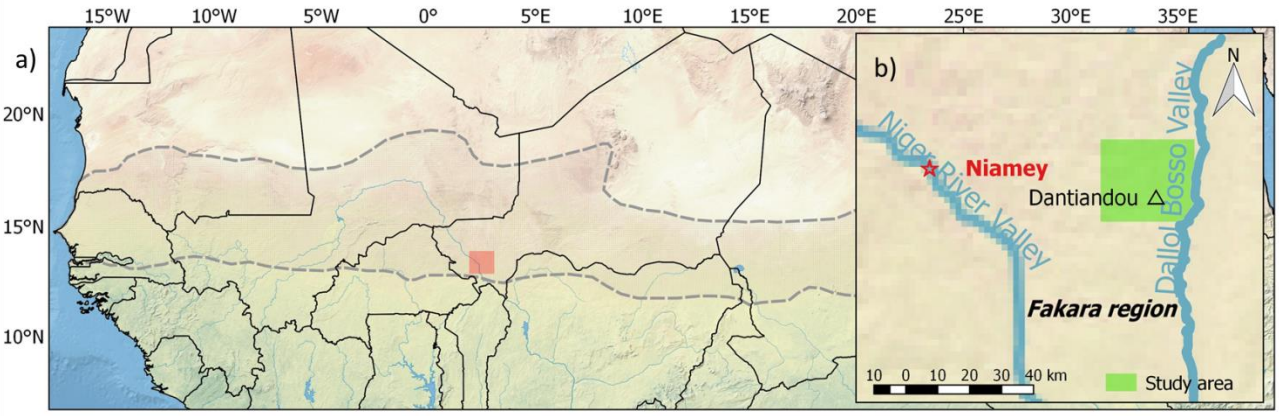

Fig. 1. a) The location of the Fakara region in Niger (red block) within the Sahelian delineation (dashed lines). b) The study area (green block: latitude North 13.40-13.57, longitude East 2.58-2.82) is located in the Fakara region.

2.2 Phenological characteristics of cropped and fallowed fields

In the Sahel, rainfed crops, dominated by pearl millet and sorghum, are sown with the first rains from late May to late July (Osbahr, 2001). The main cereal crop is often associated with secondary crops such as cowpea, roselle (Hibiscus sabdariffa), and sesame (Ickowicz et al., 2012). Annual

herbaceous vegetation, including weeds and crops, germinates within a week. After germination, weeds are suppressed during the early growing season (from two weeks after sowing until late July). Due to the weeding practice, bare soil dominates in cropped fields in the early growing season while herbaceous vegetation continues to grow in fallows and rangelands. By late August and September, green vegetation cover becomes denser in cropped fields because of the rapid growth of the crops. After the crops have matured, the harvest (only the panicles in the case of cereals) normally begins gradually, intensifying from mid-October to late November. The shape of the cropped fields is often irregular and the size of the fields varies from a few tenths of hectares for the manured fields close to villages or camps to a few hectares for the unmanured fields further away from the villages (Minet, 2007).

In contrast, fallowed fields are covered by herbaceous vegetation and scattered trees as well as a bush and shrub layer that increases in cover with the age of the fallow (Cisse, Hiernaux, & Diarra, 1993). Fallow field vegetation is dominated by annual herbaceous plants (long cycle grasses and short cycle dicotyledons). Both germinate with the first rains and flower from late August to mid-September, driven by the sensitivity to the photoperiod (Penning de Vries & Djitèye, 1982). The herbaceous vegetation wilts soon after seed maturation from mid-September to mid-October. Although the annual herbaceous layer quickly turns into straw, the soil of fallows remains covered with litter for most of the dry season (Bielders, Rajot, & Amadou, 2002). Farmers decide which fields to fallow and for how long by assessing soil fertility, but also by considering the availability of labor for weeding and the accessibility to land for cropping. In Fakara, the landscape was converted from a Sahelian savanna to largely eroded agricultural/agroforestry parkland during the 20th century. The native savanna on the cultivable soil, which covered a sizeable portion of the lands in the 1950s, gradually disappeared in the late 1960s (Hiernaux & Ayantunde, 2004). The fields that are not manured are frequently cultivated, typically for five years with alternate years of

fallow, typically for three years (Hiernaux & Turner, 2002). There is a transition from fallowed fields to native Sahelian savanna if a field is left fallow for over 15 years (Hiernaux et al. 2009).

3. Materials and methods

This research is based on data and methods that are sub-divided into three steps (Fig. 2): (1) Cropped and fallowed fields were sampled using land use/cover records from field observations and satellite imagery at high spatial resolution (SPOT and Landsat; 10-30 m). (2) The intra-annual seasonal NDVI signatures (NDVI seasonal metrics) of cropped and fallowed fields were extracted from MODIS data at a lower spatial resolution (250 m resolution) using the samples generated from (1). (3) On the basis of the NDVI 250 m resolution seasonal metrics, cropped and fallowed fields were mapped for each year from 2000 to 2014 using a fuzzy-c means algorithm. Finally, the dynamics in cropped and fallowed fields were linked to NDVI trends for the study area.

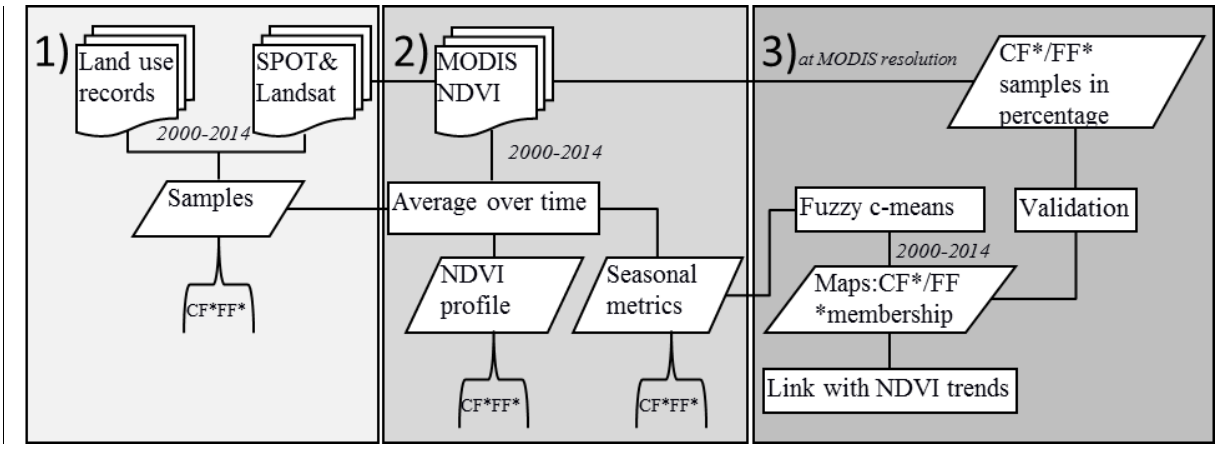

Fig. 2. Flow chart of the methods applied in this study (CF*FF*: the two field types of cropped and fallowed fields). 1) Sampling the two field types; 2) temporal profile extraction; 3) mapping the cropped/fallowed fields and analyzing the relation to NDVI trends.

3.1 Data

3.1.1 Land use records from field observations

Validation and interpretation of the satellite observed trends are generally limited due to the lack of long-term continuous field measurements (Dardel et al., 2014; Mbow, Fensholt, Nielsen, & Rasmussen, 2014). The long-term monitoring (since 1994) of land use/cover from the Fakara region, available for this study is therefore quite unique for the Sahel (from 1994 to 2006 within the framework of International Livestock Research Institute (ILRI) (Hiernaux & Ayantunde, 2004; Hiernaux et al., 2009) and from 2006 to the present under the AMMA-CATCH observatory activities (African Monsoon Multidisciplinary Analysis-Couplage de l'Atmosphère Tropicale et du Cycle Hydrologique) (Cappelaere et al., 2009; Hiernaux et al., 2009).

Initially, 48 sites of cropland (24) and fallow and uncultivable rangeland (24) were selected in 1994 to study crop-livestock interactions in mixed farming systems within the ILRI framework (Hiernaux & Ayantunde, 2004). Systematic field surveys have been undertaken on an annual basis at the end of growing season (October), providing a continuous data record of land use/cover from 1994 to 2015. The land use/cover has been recorded repetitively over the years along transects as cropland, fallow, or uncultivable rangeland. Transects were 100 m long in cropland (cropped fields) and 200 m long in fallow fields and uncultivable rangeland; location coordinates were recorded using non-differential GPS. Due to the frequent changes in land use (except three sites of uncultivable rangeland and five sites of manured cropland with no change in land use), the number of monitored sites was extended over time to maintain a balance between on the one hand, the number of cropland sites and on the other, the number of sites of fallow and uncultivable rangeland together. Historical land use/cover of the added sites was filled in on the basis of farmers' recall (Hiernaux et al., 2009). To match the first year of acquisition of MODIS scenes, only land use/cover records collected from 2000 onwards were used in the study, for an updated total number of 72 sites.

A mosaic landscape of three land use/cover types can be found in the region (Fig. 3): cropped fields, fallowed fields, and non-cultivable rangeland. The remains of native vegetation consist of 'tiger

bush' (D'Herbès, Ambouta, & Peltier, 1997), which grows on the uncroppable ferricrete plateau. The linear thickets of tiger bush and the bare soil impluvium in between them have a distinctive phenology and radiometric signature (Hiernaux & Gérard, 1999). Due to the focus on studying cropped and fallowed fields on sandy cultivable land, the uncultivable rangelands, together with water bodies and villages, were masked out and disregarded from the analysis using a detailed mask based on SPOT data (unpublished) corresponding well to the mask produced by Lambert et al, 2014, based on PROBA-V data.

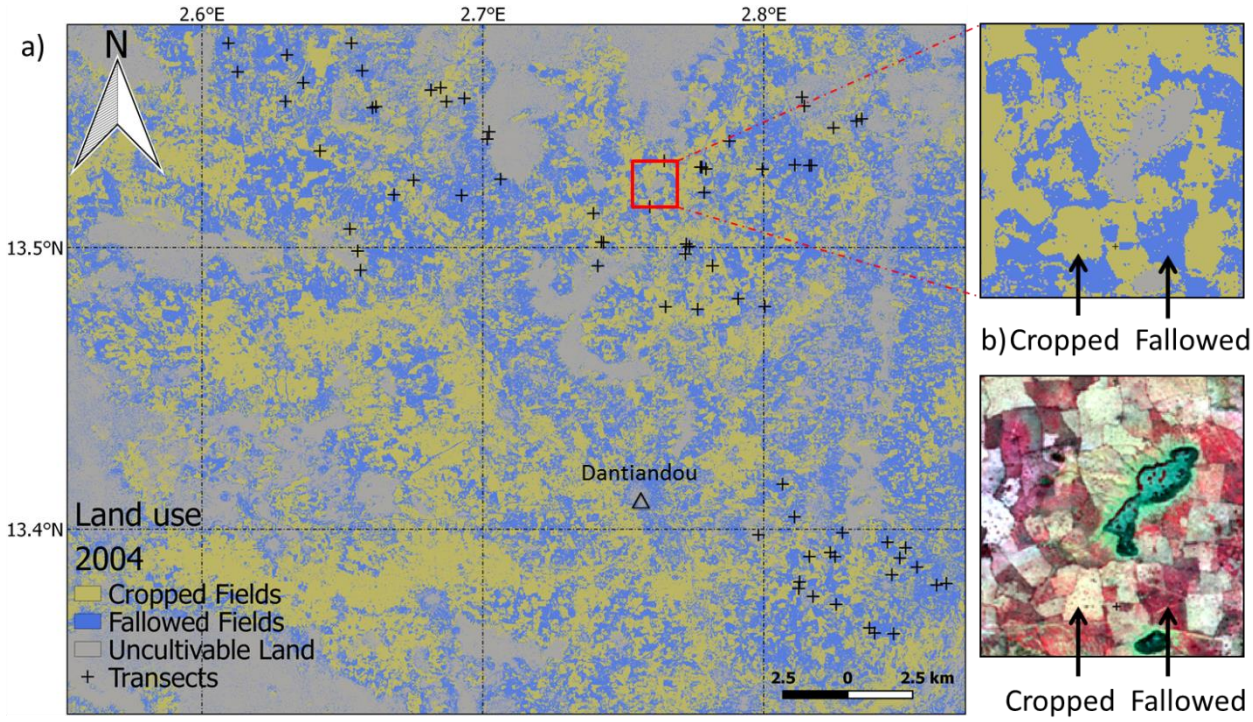

Fig. 3. a) Land use/cover map showing the location of the 72 transects for the vegetation surveys (Hiernaux et al., 2009). A supervised classification was done using a SPOT 10 m image from September 28, 2004. b) The map insert shows the same SPOT image in a false color composition (patches of bright white and dark red represent cropped and fallowed fields, respectively).

3.1.2 SPOT and Landsat images

Data from the SPOT and Landsat archives were combined to achieve annual coverage of cloud-free end of growing season images for the study area from 2000 to 2014 (Table 1). As no images of good quality were available for 2011, this year was omitted from the further analyses. We used SPOT 4 and 5 multispectral bands with spatial resolutions of 20 m and 10 m, respectively, acquired from the European Space Agency through Airbus Defence and Space (http://www.geo-airbusds.com/). The acquired images were radiometrically corrected and georeferenced to match a standard map projection (UTM 31/WGS84) based on ground truth points. Systematically corrected Landsat Surface Reflectance High Level Data Products were ordered from the United States Geological Survey through EarthExplorer (http://earthexplorer.usgs.gov/). For 30 m resolution Landsat 4-5 Thematic Mapper (TM) or Landsat 7 Enhanced Thematic Mapper Plus (ETM+) data, surface reflectance data came already pre-processed using the Landsat Ecosystem Disturbance Adaptive Processing System (LEDAPS), including the atmospheric and geometric correction.

Table 1. Selected SPOT and Landsat imageries.

Mission	Acquired date	Resolution
Landsat 5	2000.09.24	30 m
Landsat 5	2001.09.11	30 m
SPOT 4	2002.09.28	20 m
SPOT 4	2003.09.26	20 m
SPOT 5	2004.09.28	10 m
SPOT 4	2005.09.28	20 m
SPOT 4	2006.09.23	20 m
SPOT 4	2007.09.27	20 m
SPOT 5	2008.11.20	10 m
SPOT 4	2009.09.08	20 m
SPOT 5	2010.09.21	10 m
SPOT 5	2012.09.08	10 m
Landsat 8	2013.10.06	30 m
Landsat 8	2014.09.23	30 m

3.1.3 MODIS NDVI data

To form a dense time series, a MODIS NDVI time series at 250 m spatial resolution is deemed more appropriate than the higher spatial resolution data such as Landsat and SPOT imagery (≤ 30 m) due to the lack of cloud-free imageries during the short and intermittent rainy/growing season characterizing the Sahel. The newly released MODIS Surface Reflectance product (MOD09Q1) collection 6 from the Terra platform (www.reverb.echo.nasa.gov) was used to derive an NDVI time series at 250 m resolution for 2000 to 2014. MOD09Q1 provides estimates of surface reflectance for two spectral bands (Red band 1: 620-670 nm; NIR band 2: 841-876 nm). The MOD09Q1 8-day product was selected because it contains the best possible level 2 (L2G) daily observations during an eight-day period (Vermote, El Saleous, & Justice, 2002; Gao, Masek, Schwaller, & Hall, 2006), which was found to be optimal for capturing the differences in temporal changes for cropped and fallowed fields.

3.2 Sampling cropped and fallowed fields from SPOT/Landsat data

Using the SPOT/Landsat dataset (Table 1), a method was applied to locate both cropped and fallowed fields covering sufficiently large areas to extract the NDVI signature from 250 m MODIS pixels. (1) Maximum likelihood classification (MLC) was performed on each image (representing individual years) to obtain three classes (cropped fields, fallowed fields, and uncultivable land). This was done using the land use/cover records of the transects (ground observations), which were converted from lines (100 m/200 m) to polygons (200 m×100 m/300 m×100 m) by buffering 50 m in each direction. (2) Filtering with the majority vote was applied on the classified maps to remove isolated pixels regarded as noise by replacing pixels in clusters of pixels (3×3 pixels) on the basis of the majority of their contiguous neighboring pixels.

Cropped and fallowed fields were sampled using an interactive visualization of the classification and SPOT/Landsat image in a false color composition. Given the challenging ground reality of

241 fields, in this way, both field samples and classified maps were evaluated visually using ground
242 truth knowledge (Fig. 3b). For each year, 20 cropped fields and 20 fallowed fields were sampled to
243 meet the requirement that each sample should cover at least one 250 m MODIS pixel.

244 *3.3 Extraction of seasonal NDVI signatures for cropped and fallowed fields*

245 The NDVI signatures of cropped and fallowed fields for each year were composed of 46 NDVI
246 values (using the 8-day temporal resolution MODIS product), each calculated by averaging the
247 NDVI values of the above mentioned 40 samples of cropped (20) and fallowed fields (20) generated
248 for a given year. The entire study period includes wet and dry years, making single-year seasonal
249 NDVI signatures less representative. To have a robust seasonal NDVI signature, the final NDVI
250 profile for cropped and fallowed fields was generated by averaging the derived seasonal NDVI
251 signatures of the years of the entire study period (Fig.5a).

252 Seasonal metrics were extracted on an annual basis from the MODIS NDVI time series using the
253 Timesat software (http://web.nateko.lu.se/timesat/timesat.asp) (Jönsson & Eklundh, 2004), which is
254 a widely-used tool to analyze satellite time series in relation to vegetation phenology (Brandt et al.,
255 2016; Diouf et al., 2015; Fensholt et al., 2015; Olsson et al., 2005; Wang et al., 2015). The seasonal
256 metrics (Table 2) were computed on the basis of the fitted NDVI time series using a Savitsky-Golay
257 filter. The start and end of the season were estimated by setting a user-defined fraction of the
258 seasonal amplitude, based on relevant knowledge of *in situ* seasonality. In this study, the start of the
259 season was set to 20% of the seasonal amplitude to capture the general vegetation growing period
260 (from mid-July to end of October) estimated from field experiences (section 2.2). The end of the
261 season was defined using the criterion of 45% of the seasonal amplitude, approximately
262 corresponding to the end of vegetation growing season, when the senescence of herbaceous

vegetation occurs and only woody plants remain green with active photosynthesis (Brandt et al., 2016).

Table 2. Satellite-derived seasonal NDVI metrics used in this study.

Variable	Definition	Reported Unit
Amplitude	Difference between maximum and base value	NDVI unit
Base value	Mean of minimum NDVI values before sos and after eos	NDVI unit
End of season (eos)	Ending point of the growing season (45% of amplitude)	Day of year
Length of season	Number of days from sos to eos	Number of days
Maximum value	Highest value of a year	NDVI unit
Right derivative	Rate of decrease at the end of the season	NDVI unit/Time unit^{-3}
Small integral	Integral from sos to eos but above base value	NDVI unit
Start of season (sos)	Starting point of the growing season (20% of amplitude)	Day of year

3.4 Cropped and fallowed fields separation from temporal NDVI signatures

Accurate wall-to-wall separation of the 'cropland' into cropped and fallowed fields using Timesat-derived seasonal metrics (see Section 3.3) can be difficult due to the presence of mixed pixels composed of both cropped and fallowed fields (approximate $\leq$ 1 ha) at the spatial resolution of MODIS data (approximate $\geq$ 6 ha). Also, the development of training sets for supervised image classifiers without any *a priori* knowledge is another challenging task, as agricultural fields change dynamically over time from cropped to fallowed fields and back again. Therefore, we applied a simple and robust unsupervised method for this step, which reports the membership of mixed pixels to cropped/fallowed fields in a gradation of percentage values and does not require training data (Ghosh, Mishra, & Ghosh, 2011; Zhang, Du, Li, Fang, & Ling, 2014). The method is an unsupervised fuzzy c-means (FCM) algorithm (Bezdek, Ehrlich, & Full, 1984), which is a non-parametric fuzzy clustering (classification) technique appropriate to separate overlapping clusters (classes) (Mather & Tso, 2016).

Upon selection of the desired number of clusters for the FCM algorithm, the belonging of a pixel to a cluster (membership) is derived through the iterative optimization of an objective function, which

calculates the Euclidean distance of each pixel from the center of a given cluster. Without *a priori* training data for the defined clusters, the first iteration starts with an initial guess of the memberships of all pixels and stops when the iteration reaches either the number of times or the accuracy pre-defined by users. The membership value ranges from 0 to 1, indicating the ratio of the class to each of the defined classes (e.g., for two classes of cropped and fallowed fields, a pixel with a membership value of 0.3 for cropped fields will have a membership value of 0.7 for fallowed fields). We used *scikit-fuzzy* (http://pythonhosted.org/scikit-fuzzy/overview.html), which is a fuzzy logic toolbox for Python, implemented with an FCM clustering algorithm (Ross, 2004). Following the design of the analysis, the number of clusters (*c*) should be two (cropped and fallowed fields). However, by including only two clusters, the center of a cluster determined by the unsupervised algorithm will locate in the space of mixed pixels (Fig. 4a) and the algorithm will assign the same membership values to pixels having the same Euclidean distance to the center of cluster. This causes the incorrect clustering of mixed pixels to the endmembers, which represent the pure cropped and pure fallowed fields in a spectral image. To circumvent this, the approach can be optimized in two steps using different settings for the number of clusters (Fig. 4b). Firstly, we applied the FCM algorithm on input images of the selected seasonal metrics to 100 clusters to generate the center of two "pure" clusters of cropped and fallowed fields (endmember sets). Secondly, we re-applied the FCM algorithm to the same input images using the extracted endmember sets to generate the cropped/fallowed field membership maps. Three additional parameters were set: maximum number of iterations (maxiter) = 1000, accuracy (error) = 0.005, and weighting parameter (m) = 2. The weighting parameter is an exponent factor in the algorithm to control the amount of fuzziness in the clustering process; the most widely used values are in the range of 1.25 to 2 (Ross, 2004). The analysis was applied at extent of the detailed mask extent (see section 3.1.1) reported as the study area in Fig.1 b.

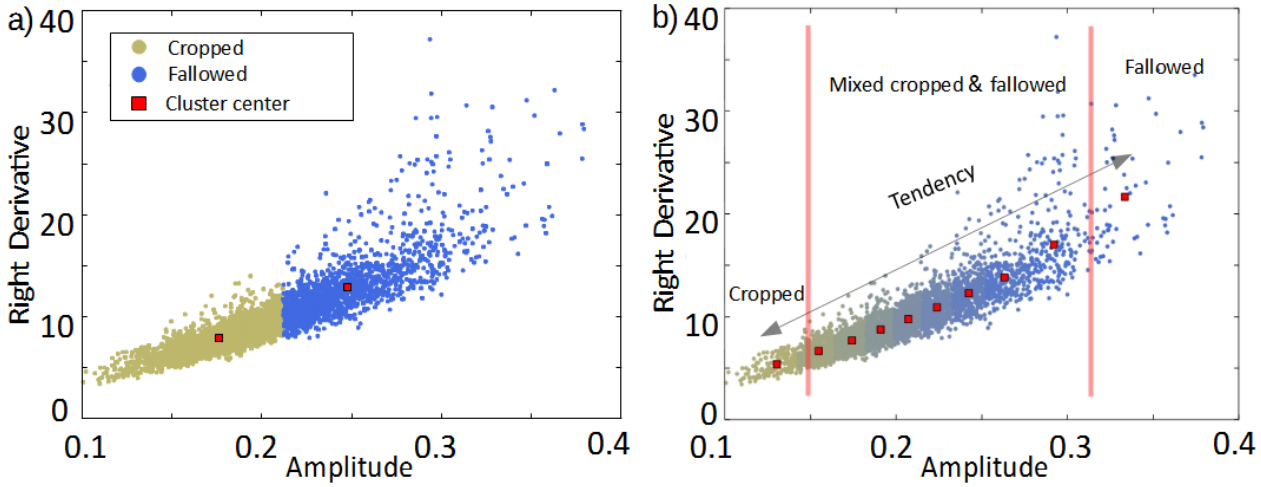

305

306 **Fig. 4.** Scatter plots illustrating the locations of unsupervised FCM generated clusters (red squares). Examples of a) 2
307 clusters and b) 10 clusters using the inputs of amplitude and the right derivative of the year 2004. A larger number of
308 clusters will facilitate extraction of endmembers for pure cropped and fallowed fields.

309 *3.5 Validation*

310 In several land use/cover mapping studies, the membership value has been used as a proxy for the
311 fractional coverages of land use/cover classes on the ground (Foody, 2000; Wang, 1990). It is thus
312 possible to validate the membership of cropped and fallowed fields by comparing with the
313 corresponding percentage of cropped and fallowed fields estimated by visually identifying and
314 digitizing the classes using contextual information, such as patterns, texture, and colors from false
315 color composite Landsat/SPOT imagery. We digitized the fallowed fields in single MODIS 250 m
316 pixels using the available four years of SPOT 5 imagery (2004, 2008, 2010, and 2012 (Table 1))
317 (spatial resolution of 10 m). For each of the four years, the size of 50 validation samples,
318 corresponding to a MODIS pixel size, was randomly generated and the fallowed fields in each
319 sample were digitized. The proportion of fallowed fields in each 250 m sample was further
320 calculated by dividing the area of the digitized fallowed fields by the area of one MODIS pixel. The
321 accuracy of the membership maps was evaluated through the strength (correlation coefficient), the

differences (root-mean-square error), and the significance level of linear association between fallowed field membership and the percentage of fallowed fields.

3.6 Linking cropped and fallowed fields with NDVI trends

To analyze the NDVI trends in relation to land use/cover changes, a time series of annual membership was generated (2000-2014). Temporal trends analysis was applied using a linear regression model to generate the pixel-wise slopes of annual NDVI sum and annual field membership. The slope values were standardized for comparison. Furthermore, the total cropped/fallowed area for each year was calculated by multiplying the cropped/fallowed field membership values with the area of one MODIS pixel and summing the cropped/fallowed field areas of all pixels. The standardized slope, P value, and standard deviation (SD) of the cropped/fallowed area were extracted for further statistical analysis and compared with commonly used time-series NDVI metrics (annual NDVI sum, rainy season NDVI sum (July, August and September), small integral, large integral), and annual rainfall sum (extracted over the Niamey Square Degree from 2000 to 2012 collected by AMMA-CATCH).

4. Results

4.1 Seasonal NDVI signatures of cropped and fallowed fields

A total area equal to the size of 5,000 MODIS pixels was sampled and averaged for cropped and fallowed fields over the period of study. Over the dry season (November-June), we observed that fallowed fields had a slightly higher NDVI (~0.02) than cropped fields (Fig. 5a). During the rainy season, fallowed fields had a higher maximum NDVI (~0.1) than cropped fields. Also, the NDVI of fallowed fields decreased faster than that of cropped fields after the rainy season. In all years, fallowed fields had a higher annual mean NDVI than cropped fields (Fig. 5b). For 11 out of 15

years, all 8-day composite values (N = 46) of the averaged fallowed fields NDVI are higher than cropped fields (for 2003 (N = 44), 2010 (N = 44), 2012 (N = 44) and 2014 (N = 45)).

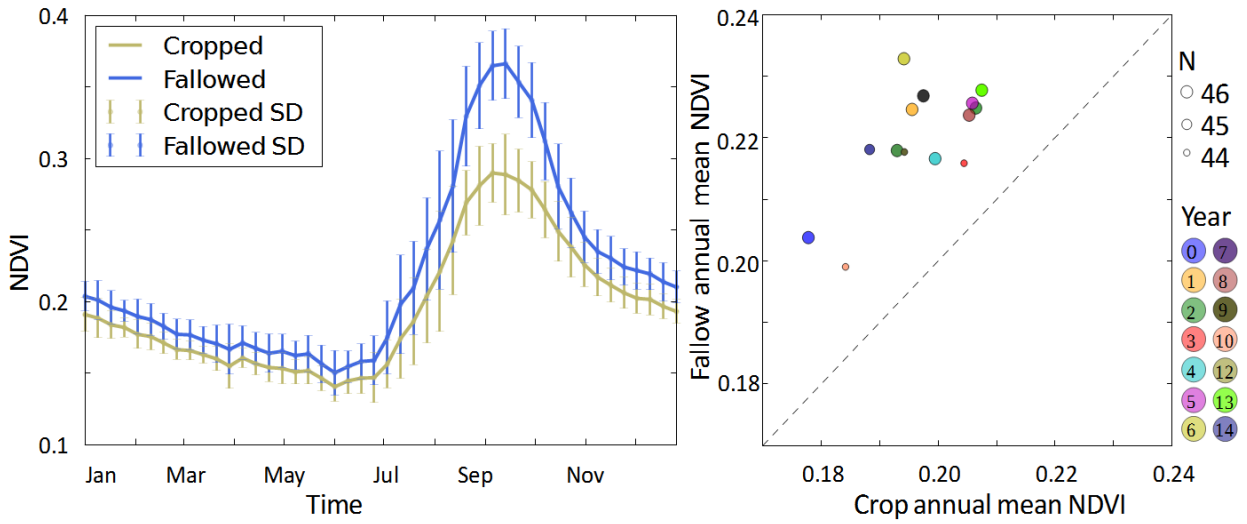

Fig. 5. a): Intra-annual NDVI profiles averaged for all cropped/fallowed fields between 2000 and 2014. b): Scatter plot between the annual NDVI average of cropped and fallowed fields. Number (N) of MODIS 8-day composite values (per year) of higher averaged NDVI of fallowed fields than of cropped fields are indicated by the size of the circles.

The fallowed fields were found to have a higher amplitude, base value, maximum, right derivative, and small integral than cropped fields and the end of season and length of season of cropped fields are later and longer, respectively, than those of fallowed fields, averaged over all years (Fig. 6a). A highly significant difference between cropped and fallowed fields was found for all these metrics ($P<0.01$), except that the length of season was found to be slightly less separable ($P<0.05$). No clear difference was detected for the determination of the start of season ($P > 0.05$).

To avoid the problem of model overfitting, only a limited number of metrics were selected as inputs for final fuzzy c-means clustering. The selection of metrics was based on the significance level (P), metric robustness, and level of phenology information content. The amplitude (2^{nd} highest P value) was selected together with the right derivative (4^{th} highest). The selection of amplitude over maximum (1^{st}) and base value (3^{rd} highest) was deemed appropriate because amplitude combines

information on both other metrics. Amplitude and right derivative were found to be significantly different ($P < 0.01$) between cropped and fallowed fields for each single year (Fig. 6b).

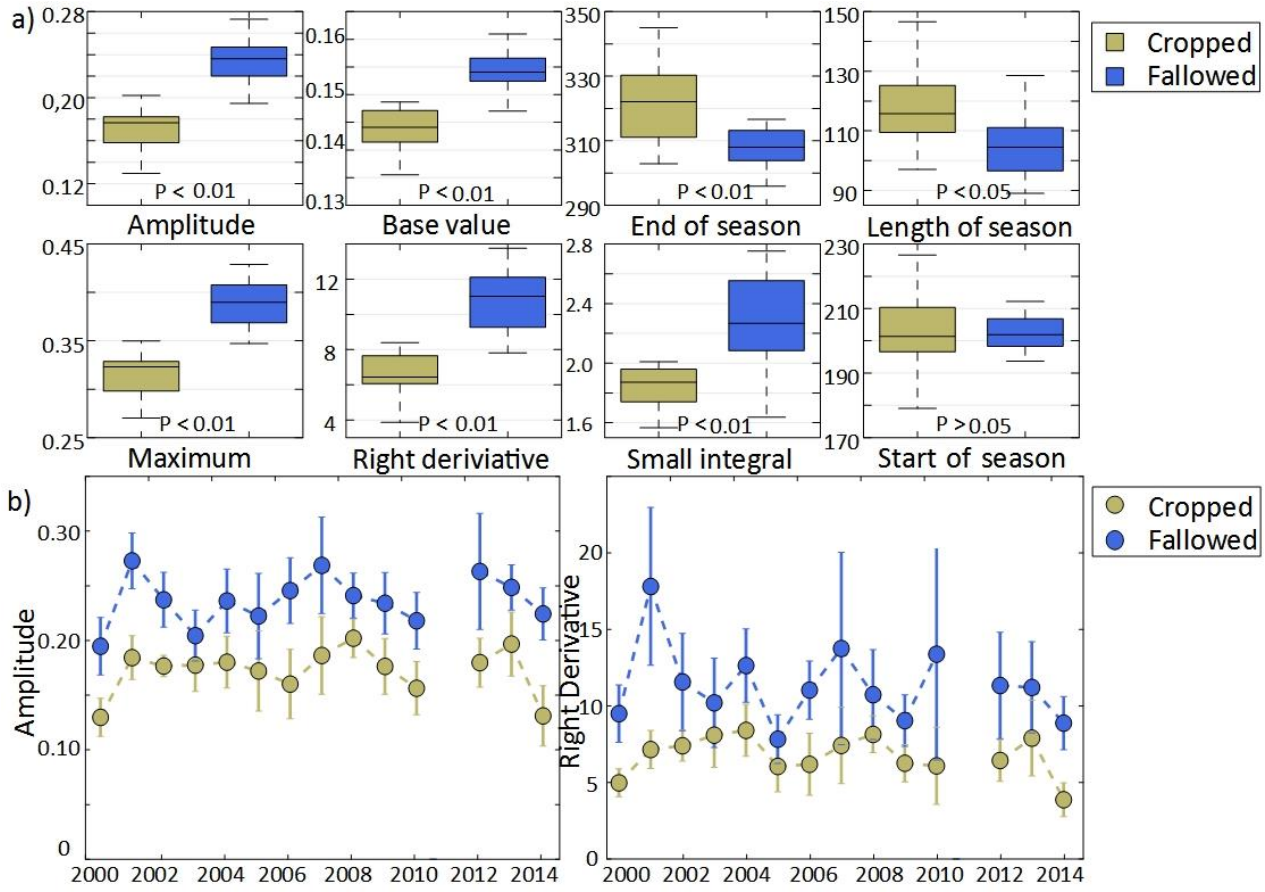

Fig. 6. a) Box plots comparing NDVI metrics for cropped and fallowed fields averaged over the period of analysis (2000-2014). b) Plots showing the yearly difference of amplitude (left) and right derivative (right) between cropped and fallowed fields. The standard deviations shown correspond to the variability between samples.

4.2 Separation between cropped and fallowed fields

The fuzzy classifier (Fig.7) captures very well the spatial distribution shown in Figure 3 (classification based on SPOT 10 m, 2004). Higher concentrations of MODIS pixels with a high fallow membership (blue) are found in the northern part of the study area and higher concentrations

of pixels characterized by a high crop membership can be observed in the southwestern part of the region (Fig. 7).

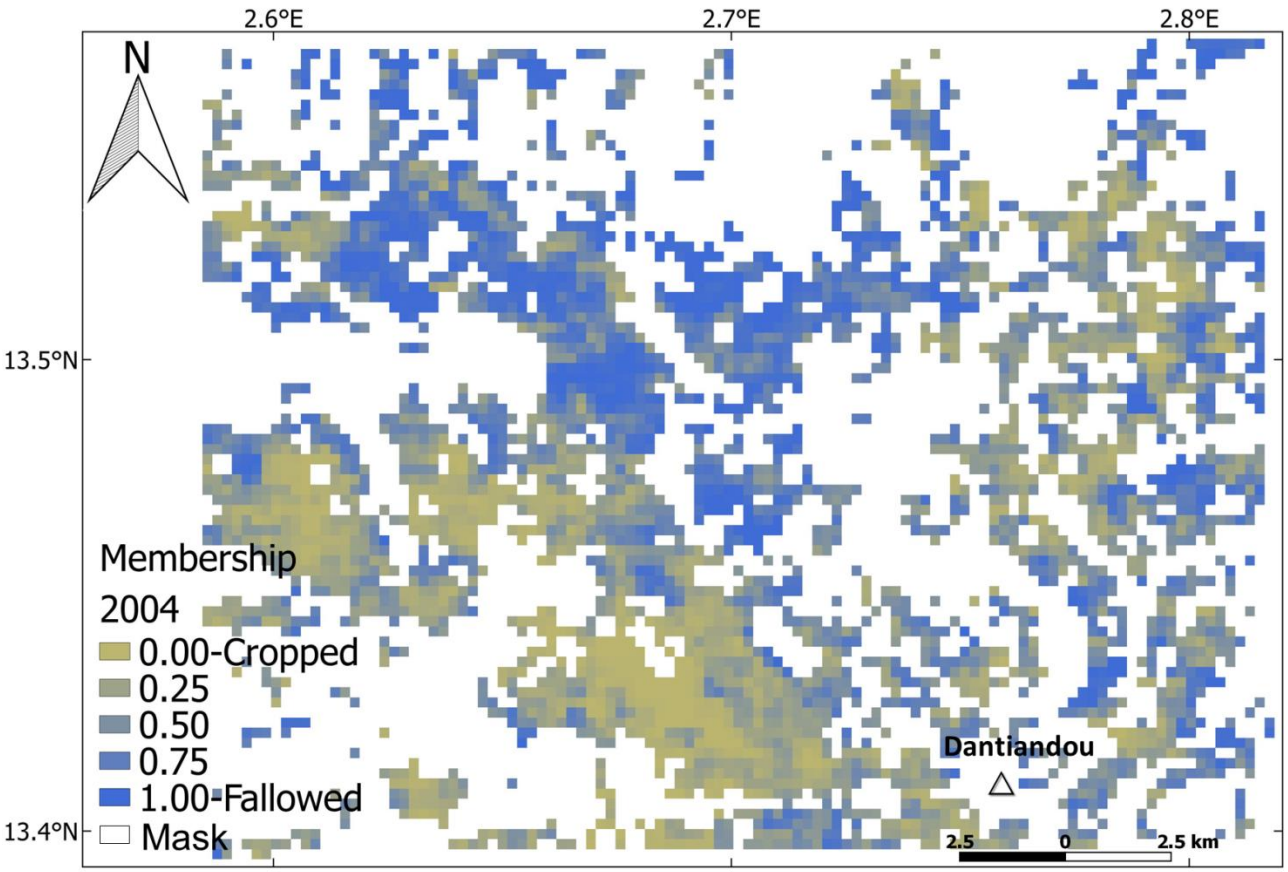

Fig. 7. Cropped/fallowed field membership map of 2004 using MODIS 250 m resolution seasonal NDVI metrics inputs (amplitude and right derivative).

4.3 Validation results

The correlation coefficients (R) between FCM membership and fallow percentage range from 0.72 to 0.81 ($p < 0.01$) for the four validated years, indicating an overall good fit (Fig. 8). The error rates for predictions (RMSE) are low, ranging from 19% to 23%. An underestimation of the fallowed field percentage is observed for 2008 and 2012. The fallowed field percentages of 2004 and 2010 were slightly underestimated for MODIS pixel size samples with a larger percentage of cropped area and overestimated for the samples with a larger percentage of fallowed area.

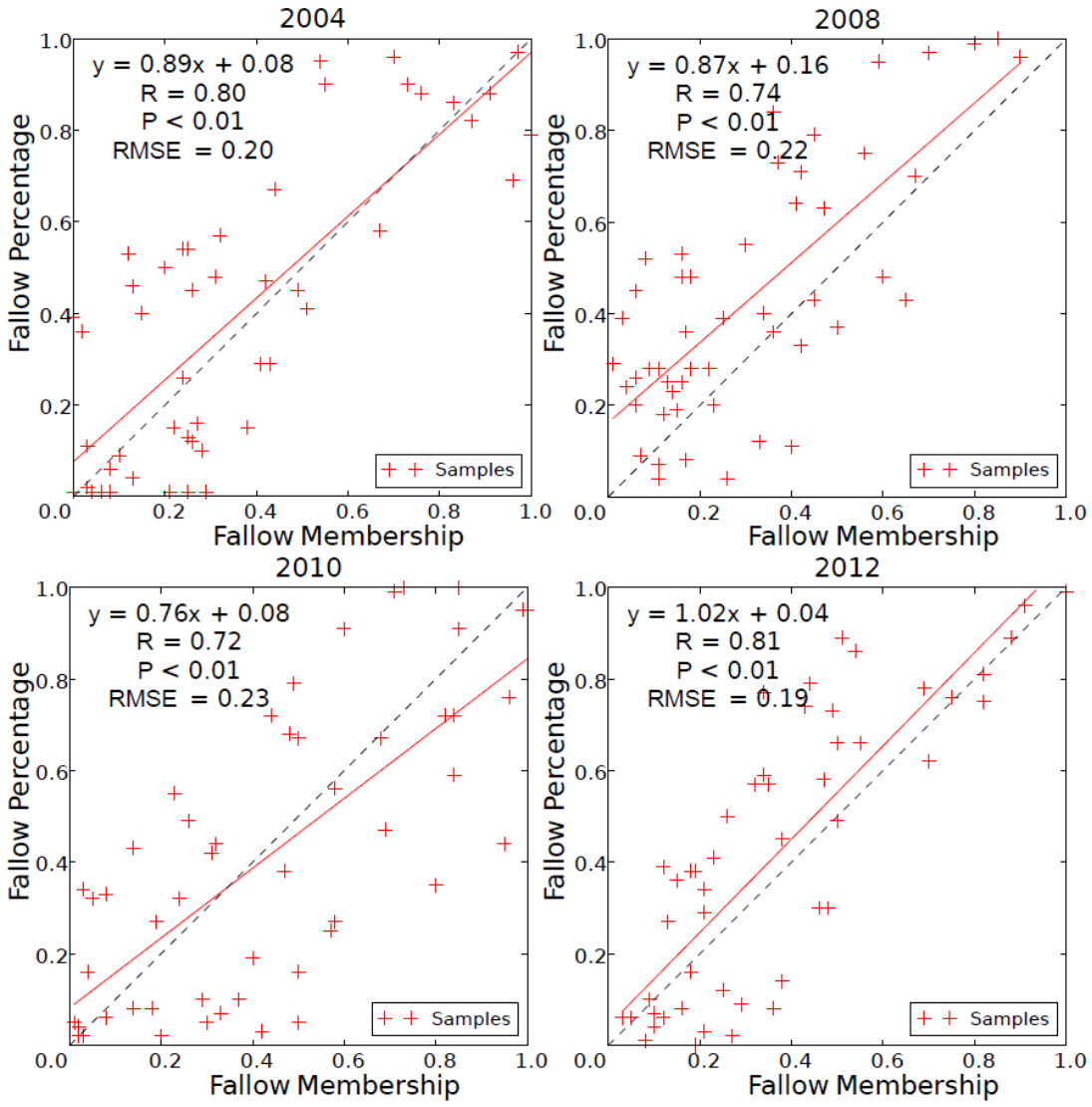

Fig.8. Linear regression between FCM membership and fallow percentage (derived from digitalizing SPOT 10 m imageries), plotted for four years (2004, 2008, 2010, and 2012).

4.4 Trend analysis

Negative trends in cropped/fallowed field membership are observed in the northern and central part of the study area (Fig. 9a), indicating an increase in the area of cropped fields from 2000 to 2014. Positive trends, associated with an increase in the fallowed area over time, are mostly seen in the southeastern part of the region. Compared with the slope map of annually summed NDVI (Fig. 9b), both the negative and positive trends of NDVI display a similar spatial pattern to cropped/fallowed

393 field membership. The slopes of NDVI and cropped/fallowed field membership are highly
394 correlated, with a correlation coefficient (R) of 0.8 ($p < 0.01$) (Fig 9c).

395 The overall trend in NDVI for the Fakara study area is negative for all summed NDVI metrics
396 commonly used for trend analysis in the period 2000-2014 (Fig. 9d and Table 3). No trends are
397 found to be significantly negative, which is primarily due to the exceptionally low NDVI values for
398 the first year of analysis (2000) caused by low rainfall (Hiernaux et al., 2009). The trend of the
399 annual NDVI sum (slope = -0.083; P = 0.19) is stronger and more significant than that of the small
400 integral (slope = -0.057; P = 0.38). Starting the analysis in 2001 (excluding the abnormally dry year
401 of 2000) would cause the negative trend of the annual NDVI sum to be highly significant (slope = -
402 0.150; P = 0.014) (Table 3). In contrast, there is a significant positive trend in the total cropped area
403 ($p < 0.1$) and a corresponding decrease in total fallowed area. As no significant trend in annual
404 rainfall was observed over the 15 years studied, it is unlikely that rainfall is responsible for the
405 negative NDVI trend, pointing towards changes in the cropped area as a main driver for the
406 observed trend. Although the timing and frequency of rainfall can have a significant impact on
407 vegetation productivity, it is beyond the scope of analysis in the current study.

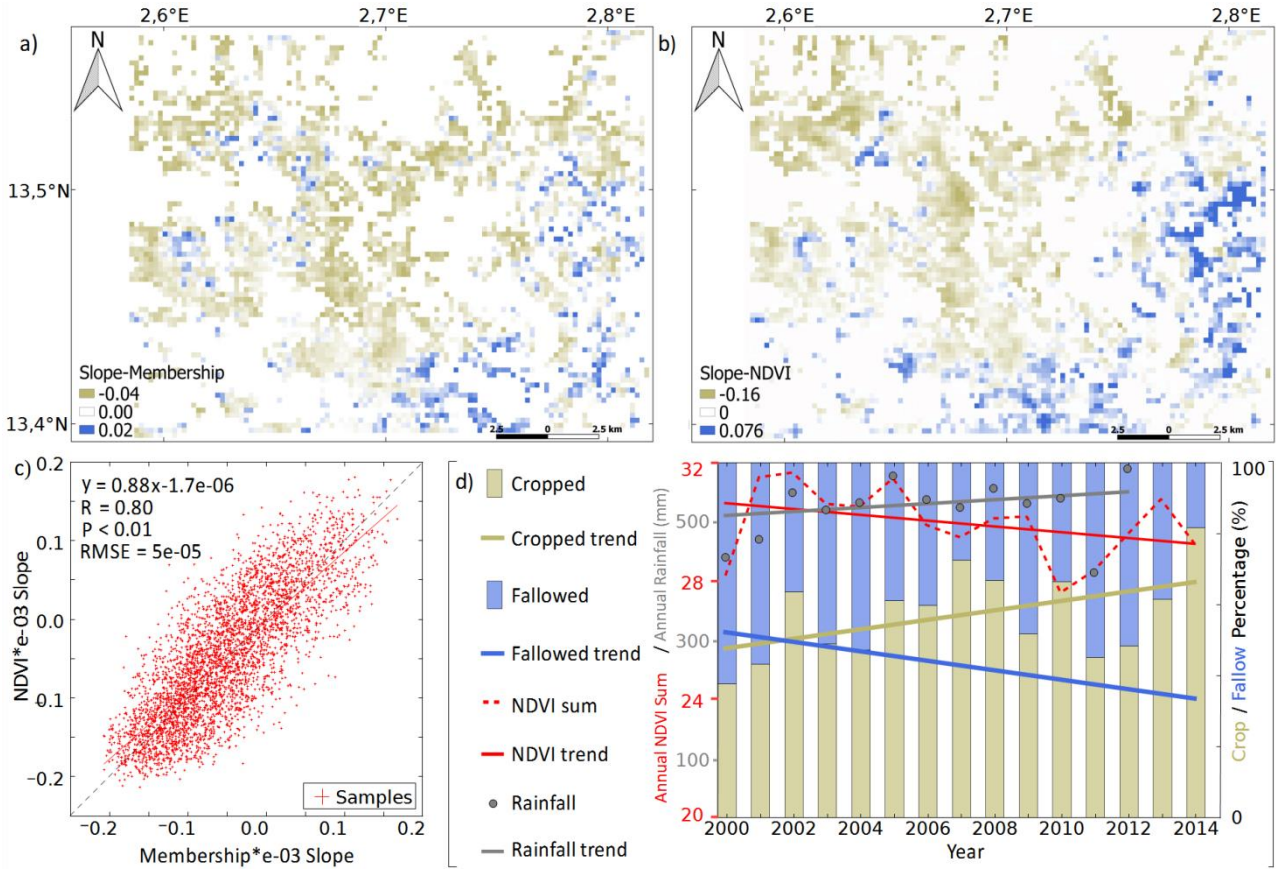

408

409 **Fig. 9.** a) Slope values from linear regression trend analysis of cropped/fallowed field membership maps (2000-2014).
410 Positive slope values mean a direction of change towards more fallows, b) slope values from the linear regression trend
411 analysis of MODIS annual NDVI sum (2000-2014), c) scatter plot showing the relation between slope values of
412 cropped/fallowed field membership and annual NDVI sum, and d) bar plot showing the percentage of cropped and
413 fallowed areas in the Fakara study area. Linear trends are shown for cropped fields, fallowed fields, annual NDVI, and
414 rainfall sum.

415 **Table 3.** Standardized coefficients of linear regression analysis (2000-2014).

Variables	Cropped fields	Fallowed fields	NDVI metrics					Rainfall
			Annual sum		Small integral	Large integral	JAS sum	annual sum
			2000-2014	2001-2014				
Slope	0.113	-0.113	-0.083	-0.150	-0.057	-0.042	-0.047	0.068
P value	0.065	0.065	0.192	0.014*	0.380	0.522	0.472	0.403
SD	0.056	0.056	0.060	0.052	0.062	0.063	0.063	0.078

416 * Significant at p<0.05

417

5. *Discussion*

This study has demonstrated that cropped and fallowed fields are characterized by different seasonal NDVI metrics, which has important implications for the interpretation of greening and browning trends in the Sahel based on satellite time series (Dardel et al., 2014; Kaptué, Prihodko, & Hanan, 2015). Cropped fields have been shown to have a significantly lower summed NDVI than fallowed fields for the study area, and if cropped and fallowed fields are merged into one land use/cover class, the corresponding NDVI trends must be interpreted with caution.

5.1 Linking changes in cropped and fallowed field areas to NDVI trends

For the study area in Fakara, an overall negative NDVI trend was observed in the period 2000-2014, and at the same time we also observed an increase in cropped areas. Although this is in line with Dardel et al. 2014, who related the negative NDVI trend in Fakara to a decrease in field measured herbaceous mass (1994-2011), the period of analysis is different, and Dardel et al. 2014 did not find a negative trend for herbaceous mass between 2000 and 2011. Furthermore, no trend in rainfall was observed for the time period analyzed here, which is in line with Dardel et al. 2014 and Hiernaux et al. 2016, making changes in water availability very unlikely as an explanation for the decreasing NDVI (a strong coupling between integrated NDVI and rainfall is normally observed in the Sahel (Fensholt et al., 2013; Huber et al., 2011). This points towards land use and management as explanations for the decrease in NDVI, and here we document an increase in per pixel cropped area percentages. Given the fact that all arable land was under human management in the Fakara region prior to 2000, it can be assumed that the observed change in the percentage of cropped area is caused by a change in the crop-fallow cycle towards less fallowed and more cropped fields during the period studied.

Although no greening was observed in our study area, these findings should be considered in the greening Sahel debate. Apart from the well-known influence from changes in rainfall (Dardel et al., 2014), there are two different interpretations of the causes of a positive NDVI trend in cropland areas: (1) an intensification due to increased use of fertilizers (usually organic manure on staple crops) (Hiernaux, Dardel, Kergoat, & Mougin, 2016), and (2) a change in the crop-fallow cycle of a given area with more frequent fallow years or even the complete abandonment of the cropped fields for several years. This second cause, supported by the current findings, might lead to a rethinking of several assumptions about the re-greening of the Sahel. It suggests that, in some places, the Sahel greening might not be caused by an increased agricultural productivity (Bégué et al., 2011), but rather by an abandonment of the fields, i.e., a decrease in agricultural activities. The abandonment could be caused by declining soil fertility (paradoxically leading to an increased NDVI, as savanna vegetation takes over fallowed fields), or by a diversification of livelihoods of the local people (the prolonged droughts in the 1970s and 1980s and the following dry period made cultivation a highly uncertain income, and some people abandoned their fields and sought alternative livelihood strategies (Brandt, Romankiewicz, Spiekermann, & Samimi, 2014; Rasmussen & Reenberg, 2012; Romankiewicz, Doevenspeck, Brandt, & Samimi, 2016)). Rainfall in the Sahel has increased during recent years, but inter and intra-annual variability has increased as well (Sanogo et al., 2015), and many farmers are reluctant to take this risk or have generated a different income (Romankiewicz et al., 2016). Even though fields might be abandoned or rarely used, this is likely to be missed in traditional classifications based on Landsat-like spatial resolution, which merges cropped and fallowed fields. Alternatively, it may be detected as an increase in NDVI and interpreted as an increase in agricultural productivity. Since lands that are being left for fallow over long time periods (around 15 years) tend to have vegetation similar to natural savanna, also the conversion from

savanna to (cultivated) cropland might impact NDVI trends in a way comparable to our case study area (i.e. a negative NDVI trend).

5.2 Applicability of results at the Sahel scale?

To further relate the current results to the re-greening of the Sahel, an extrapolation of our method to Sahel scale is required, which poses a number of challenges. Firstly, natural resource management is not uniform, and the method should be robust toward different land use practices. Secondly, the vegetation is adapted to the decreasing mean rainfall gradient from South to North (approximately 1 mm/km). Although rainfed cropping is only marginally practiced in the northern zones of the Sahel, it would be wise to study the cropped/fallowed differences for each rainfall zone separately. Thirdly, a frequently updated pre-classification could be necessary to separate non-arable land from potentially cropped areas to be analyzed for changes in cropped/fallowed spatio-temporal patterns. Reliable classifications across the Sahel have been deficient, but recently, a few promising approaches on cropland classifications have emerged (Lambert et al., 2016), which might be used to overcome this issue. However, these are snapshots in time, and without proper field data, which are usually scarce and not publicly available, and/or reliable and detailed classifications covering several years, validation and calibration is not possible. Finally, manured cropped fields that are sown more densely and grow more rapidly are likely to be characterized by different NDVI seasonal metrics (being more similar to fallowed fields) than unmanured cropped fields. As manured fields are usually located around villages, we masked these areas by using a buffer of 500 m around settlements, but this might be challenging at Sahel scale.

5.3 Methodological limitations

The method presented includes several assumptions/uncertainties, which also must be taken into account when applying the method at larger spatial scales and/or using it to interpret NDVI trends.

The fuzzy classification method was used to estimate the percentage of a field that is cropped/fallowed on an annual basis. However, strictly speaking, the method predicts the probability of a pixel belonging to either the crop or the fallow endmember class. While several studies have interpreted this as equivalent to percentage (Foody, 2000; Wang, 1990), it is not exactly the same unless no untrained classes are included in the analysis (Foody, 2000). Even though cropped/fallowed fields are the only two classes considered in the analysis, some uncertainty remains when applying FCM to coarser resolution imagery, which might still include untrained classes at the sub-pixel level. To improve the method, a higher spatial resolution would be advantageous, which is, however, currently not available at this temporal frequency over a longer time period. PROBA-V provides a resolution of 100 m (Lambert et al., 2016) but it is not yet available for multiple years, and the lower temporal frequency, as compared to MODIS, reduces the chance of having cloud-free images.

Disturbances by clouds have also been shown to influence the current MODIS based analysis of seasonal NDVI metrics. The start of the growing season metric (SOS), which is a period with persistent cloud cover in the Sahel (Fensholt et al., 2011), has been of limited use for our analysis, despite the expectation of a distinct difference between the green-up of crops and the herbaceous stratum of rangelands and fallows (due to the weeding of cropped fields). This is in line with Diouf et al. 2016, who did not find any significant relationship between a satellite-based metric of SOS and rangeland field data from Senegal. A newer MODIS retrieving algorithm termed MAIAC (Multi-Angle Implementation of Atmospheric Correction) can deliver more cloud-free images as compared to the standard MODIS processing (Bi et al., 2016; Lyapustin et al., 2012) and this might enable the implementation of additional seasonal NDVI metrics to improve the separability of land use/cover classes in future studies.

509 Another variable influencing seasonal NDVI metrics in general, and the SOS metric in particular, is
510 the woody vegetation, as leaves of several Sahelian woody species sprout before the wet season
511 starts and the herbaceous vegetation and crops germinate (Brandt et al., 2016). Here, we observed a
512 constant gap between cropped and fallowed fields (Fig. 5a), which might be caused by differences
513 in woody vegetation cover. Whereas most shrubs are annually coppiced in fields prior to cultivation,
514 they are left to grow in fallowed fields, leading to a higher shrub/woody plant cover. In recent years,
515 though, there have been great efforts in the Sahel to leave more trees on agricultural land
516 (agroforestry parklands) (Bayala, Sanou, Teklehaimanot, Kalinganire, & Ouédraogo, 2014), likely
517 to influence the NDVI signals of cropped fields in a different way than is observed in the Fakara
518 region (very limited agroforestry). Potential effects of Parklands on seasonal metrics should be
519 analyzed further if applying the current method at the Sahel scale. Finally, the abundance of big
520 trees in the cropped fields in proximity to the villages impacts the NDVI signal significantly.

521 ***6. Conclusion***

522 Existing land use/cover studies commonly merge cropped and fallowed fields into one class of
523 cropland/agriculture and different hypotheses have been brought forward when interpreting the
524 relation between positive NDVI trends and changes in areas under cultivation. For a case study area
525 in the southern Sahel (Fakara region, Niger) we have developed a classification approach to
526 separate cropped from fallowed fields based on the different phenological characteristics of the
527 vegetation as monitored by MODIS 250 m resolution data. Fallowed fields generally have a higher
528 NDVI and a more rapid decreasing rate (after the wet season) than unmanured cropped fields and
529 these differences in phenology were used to separate the seasonal signals of cropped and fallowed
530 fields. A fuzzy classifier (unsupervised fuzzy c-means (FCM) algorithm) was used to quantify the
531 percentage of cropped/fallowed fields for the period 2000 to 2014 on an annual scale. We observed
532 a trend toward an increase in the percentage of cropped area and a decrease in fallowed fields,

which can be interpreted as a shortening of the fallow period for this region, and at the same time, we observed a generally negative NDVI trend that was not explained by changes in rainfall over the period of analysis. In contrast to other hypotheses about re-greening being driven by an increase in organic fertilizers, we have shown here that an increasing NDVI trend might be linked to an increase in fallowed fields, caused by more frequent fallow years or land abandonment. If this result can be projected to larger areas, this has significant implications for our understanding and interpretation of greening and browning trends in relation to EO based monitoring of ecosystem services and land degradation in the arable lands of Sahel. The MODIS based development of the classification of the percentage of cropped/fallowed fields builds on their differences in seasonal metrics using an unsupervised algorithm and thereby might be applicable at the Sahel scale, although there are scale-dependent challenges to overcome in relation to differences in land use practices and annual rainfall. To further test the importance of land abandonment and intensification (both from usage of manure and from shortening fallow periods) for the observed trends in NDVI at the Sahel scale, the applicability of this phenology driven classification approach must be studied at larger scales involving a wider range of climatic conditions and human livelihood strategies.

Acknowledgments

This research is partly funded by the China Scholarship Council (CSC, number 201407650011) and partly by the Danish Council for Independent Research (DFF) Sapere Aude program: the “Earth Observation based Vegetation productivity and Land Degradation Trends in Global Drylands” project. Martin Brandt is the recipient of the Marie Sklodowska-Curie fellowship (project BICSA grant number 656564). In addition, the research benefits from the previous work performed by the International Livestock Research Institute (ILRI) and AMMA-CATCH in Niger.

555 ***References***

556 Alcantara, C., Kuemmerle, T., Prishchepov, A. V., & Radeloff, V. C. (2012). Mapping abandoned
557 agriculture with multi-temporal MODIS satellite data. *Remote Sensing of Environment*, *124*,
558 334–347. doi:10.1016/j.rse.2012.05.019

559 Anyamba, A., & Tucker, C. J. (2005). Analysis of Sahelian vegetation dynamics using NOAA-
560 AVHRR NDVI data from 1981-2003. *Journal of Arid Environments*, *63*, 596–614.
561 doi:10.1016/j.jaridenv.2005.03.007

562 Barbé, L. Le, & Lebel, T. (1997). Rainfall climatology of the HAPEX-Sahel region during the years
563 1950-1990. *Journal of Hydrology*, *188-189*(96), 43–73. doi:10.1016/S0022-1694(96)03154-X

564 Bayala, J., Sanou, J., Teklehaimanot, Z., Kalinganire, A., & Ouédraogo, S. J. (2014). Parklands for
565 buffering climate risk and sustaining agricultural production in the Sahel of West Africa.
566 *Current Opinion in Environmental Sustainability*, *6*(1), 28–34.
567 doi:10.1016/j.cosust.2013.10.004

568 Bégué, A., Vintrou, E., Ruelland, D., Claden, M., & Dessay, N. (2011). Can a 25-year trend in
569 Soudano-Sahelian vegetation dynamics be interpreted in terms of land use change? A remote
570 sensing approach. *Global Environmental Change*, *21*, 413–420.
571 doi:10.1016/j.gloenvcha.2011.02.002

572 Behnke, R., & Mortimore, M. (2016). Introduction: The End of Desertification? In: *The End of*
573 *Desertification? Springer Berlin Heidelberg*, 1-34.

574 Bezdek, J., Ehrlich, R., & Full, W. (1984). FCM: The fuzzy c-means clustering algorithm.
575 *Computers & Geosciences*, 10, 191-203.

576 Bi, J., Myneni, R., Lyapustin, A., Wang, Y., Park, T., Chi, C., … Knyazikhin, Y. (2016). Amazon
577 Forests' Response to Droughts: A Perspective from the MAIAC Product. *Remote Sensing*, *8*(5),
578 356. doi:10.3390/rs8040356

579 Bielders, C., Rajot, J., & Amadou, M. (2002). Transport of soil and nutrients by wind in bush
580 fallow land and traditionally managed cultivated fields in the Sahel. *Geoderma*, 109, 19–39.

581 Brandt, M., Hiernaux, P., Tagesson, T., Verger, A., Rasmussen, K., Diouf, A. A., … Fensholt, R.
582 (2016). Woody plant cover estimation in drylands from Earth Observation based seasonal
583 metrics. *Remote Sensing of Environment*, *172*, 28–38. doi:10.1016/j.rse.2015.10.036

584 Brandt, M., Romankiewicz, C., Spiekermann, R., & Samimi, C. (2014). Environmental change in
585 time series - An interdisciplinary study in the Sahel of Mali and Senegal. *Journal of Arid*
586 *Environments*, *105*, 52–63. doi:10.1016/j.jaridenv.2014.02.019

587 Cappelaere, B., Descroix, L., Lebel, T., Boulain, N., Ramier, D., Laurent, J. P., … Quantin, G.
588 (2009). The AMMA-CATCH experiment in the cultivated Sahelian area of south-west Niger -
589 Investigating water cycle response to a fluctuating climate and changing environment. *Journal*
590 *of Hydrology*, *375*(1-2), 34–51. doi:10.1016/j.jhydrol.2009.06.021

591 Cisse, M., Hiernaux, P., & Diarra, L. (Eds.). (1993). Integration agro-pastorale au Sahel: dynamique
592 et potentiel fourrager des jacheres. In: *Floret, C., Serpantié, G.*, 405–413..

593 D'Herbès, J.M., Ambouta, J.M.K., & Peltier, R. (1997). Fonctionnement et gestion des écosystèmes
594 forestiers contractés sahéliens. *Libbey, Montrouge London Rome.*

595 Dardel, C., Kergoat, L., Hiernaux, P., Mougin, E., Grippa, M., & Tucker, C. J. (2014). Re-greening
596 Sahel: 30 years of remote sensing data and field observations (Mali, Niger). *Remote Sensing of*
597 *Environment*, *140*, 350–364. doi:10.1016/j.rse.2013.09.011

598 De Rouw, A., & Rajot, J. L. (2004). Nutrient availability and pearl millet production in Sahelian
599 farming systems based on manuring or fallowing. *Agriculture, Ecosystems and Environment*,
600 *104*(2), 249–262. doi:10.1016/j.agee.2003.12.019

601 Diouf, A., Brandt, M., Verger, A., Jarroudi, M., Djaby, B., Fensholt, R., … Tychon, B. (2015).
602 Fodder Biomass Monitoring in Sahelian Rangelands Using Phenological Metrics from FAPAR
603 Time Series. *Remote Sensing*, *7*(7), 9122–9148. doi:10.3390/rs70709122

604 Diouf, A. A., Hiernaux, P., Brandt, M., Faye, G., Djaby, B., Diop, M., … Tychon, B. (2016). Do
605 Agrometeorological Data Improve Optical Satellite-Based Estimations of the Herbaceous
606 Yield in Sahelian Semi-Arid Ecosystems? *Remote Sensing*, 8(8), 668. doi:10.3390/rs8080668

607 Fensholt, R., Horion, S., Tagesson, T., Ehammer, A., Grogan, K., Tian, F., … Rasmussen, K.
608 (2015). Remote Sensing Time Series, *22*, 159–183. doi:10.1007/978-3-319-15967-6

609 Fensholt, R., Langanke, T., Rasmussen, K., Reenberg, A., Prince, S. D., Tucker, C., … Wessels, K.
610 (2012). Greenness in semi-arid areas across the globe 1981-2007 - an Earth Observing Satellite
611 based analysis of trends and drivers. *Remote Sensing of Environment*, *121*, 144–158.
612 doi:10.1016/j.rse.2012.01.017

613 Fensholt, R., Rasmussen, K., Kaspersen, P., Huber, S., Horion, S., & Swinnen, E. (2013). Assessing
614 Land Degradation/Recovery in the African Sahel from Long-Term Earth Observation Based
615 Primary Productivity and Precipitation Relationships. *Remote Sensing*, *5*(2), 664–686.
616 doi:10.3390/rs5020664

617 Fensholt, R., Anyamba, A., Huber, S., Proud, S. R., Tucker, C. J., Small, J., ... & Shisanya, C.
618 (2011). Analysing the advantages of high temporal resolution geostationary MSG SEVIRI data
619 compared to Polar Operational Environmental Satellite data for land surface monitoring in

620 Africa. *International Journal of Applied Earth Observation and Geoinformation*, 13(5), 721-
621 729.

622 Foody, G. M. (2000). Estimation of sub-pixel land cover composition in the presence of untrained
623 classes. *Computers and Geosciences*, *26*(4), 469–478. doi:10.1016/S0098-3004(99)00125-9

624 Fuller, D. O. (1998). Trends in NDVI time series and their relation to rangeland and crop
625 production in Senegal, 1987-1993. *International Journal of Remote Sensing*, *19*(10), 2013–
626 2018. doi:10.1080/014311698215135

627 Gao, F., Masek, J., Schwaller, M., & Hall, F. (2006). On the blending of the Landsat and MODIS
628 surface reflectance: Predicting daily Landsat surface reflectance. *IEEE Transactions on*
629 *Geoscience and Remote Sensing*, *44*(8), 2207–2218.
630 http://doi.org/10.1109/TGRS.2006.872081

631 Ghosh, A., Mishra, N. S., & Ghosh, S. (2011). Fuzzy clustering algorithms for unsupervised change
632 detection in remote sensing images. *Information Sciences*, *181*(4), 699–715.
633 doi:10.1016/j.ins.2010.10.016

634 Herrmann, S. M., Anyamba, A., & Tucker, C. J. (2005a). Recent trends in vegetation dynamics in
635 the African Sahel and their relationship to climate. *Global Environmental Change*, *15*(4), 394–
636 404. doi:10.1016/j.gloenvcha.2005.08.004

637 Herrmann, S. M., & Hutchinson, C. F. (2005b). The changing contexts of the desertification debate.
638 *Journal of Arid Environments*, *63*(3), 538–555. doi:10.1016/j.jaridenv.2005.03.003

639 Hickler, T., Eklundh, L., Seaquist, J. W., Smith, B., Ardö, J., Olsson, L., … Sjöström, M. (2005).
640 Precipitation controls Sahel greening trend. *Geophysical Research Letters*, *32*(21), 1–4.
641 doi:10.1029/2005GL024370

642 Hiernaux, P., & Ayantunde, A., (2004). The Fakara: a semi-arid agro-ecosystem under stress.
643 *Report of research activities, first phase (July 2002–June 2004) of the DMP-GEF programme*
644 *(GEF/2711-02-4516) ILRI, ICRISAT Centre, Niamey*, 1-95.

645 Hiernaux, P., Ayantunde, A., Kalilou, A., Mougin, E., Gérard, B., Baup, F., … Djaby, B. (2009).
646 Trends in productivity of crops, fallow and rangelands in Southwest Niger: Impact of land use,
647 management and variable rainfall. *Journal of Hydrology*, *375*(1-2), 65–77.
648 doi:10.1016/j.jhydrol.2009.01.032

649 Hiernaux, P., Dardel, C., Kergoat, L., & Mougin, E. (2016). Desertification, adaptation and
650 resilience in the Sahel: lessons from long term monitoring of agro-ecosystems. *The End of*
651 *Desertification? Springer Berlin Heidelberg*, 147-178.

652 Hiernaux, P., & Gérard, B. (1999). The influence of vegetation pattern on the productivity, diversity
653 and stability of vegetation: The case ofbrousse tigrée'in the Sahel. *Acta Oecologica*, 20(3),
654 147-158

655 Hiernaux, P., & Turner, M. D. (2002). The influence of farmer and pastoralist management
656 practices on desertification processes in the Sahel. *Dalhem University Press*, (Global
657 desertification: Do humans cause deserts?), 135–148.

658 Huber, S., Fensholt, R., & Rasmussen, K. (2011). Water availability as the driver of vegetation
659 dynamics in the African Sahel from 1982 to 2007. *Global and Planetary Change*, *76*(3-4),
660 186–195. doi:10.1016/j.gloplacha.2011.01.006

661 Ickowicz, a., Ancey, V., Corniaux, C., Duteurtre, G., Poccard-Chappuis, R., Touré, I., … Wane, a.
662 (2012). Crop-Livestock Production Systems in the Sahel - Increasing Resilience for Adaptation
663 to Climate Change and Preserving Food Security, *Building resilience for adaptation to climate*

change in the agriculture sector, 23, 261–294.

Jönsson, P., & Eklundh, L. (2004). TIMESAT—a program for analyzing time-series of satellite sensor data. *Computers & Geosciences*, *30*(8), 833–845. doi:10.1016/j.cageo.2004.05.006

Kaptué, A. T., Prihodko, L., & Hanan, N. P. (2015). On regreening and degradation in Sahelian watersheds. *Proceedings of the National Academy of Sciences*, *112*(39), 12133–12138. doi:10.1073/pnas.1509645112

Kaspersen, P. S., Fensholt, R., & Huber, S. (2011). A spatiotemporal analysis of climatic drivers for observed changes in Sahelian vegetation productivity (1982-2007). *International Journal of Geophysics*, *2011*. doi:10.1155/2011/715321

Lambert, M., Waldner, F., & Defourny, P. (2016). Cropland Mapping over Sahelian and Sudanian Agrosystems : A Knowledge-Based Approach Using PROBA-V Time Series at 100-m. *Remote Sensing*, 8(3), 232. doi:10.3390/rs8030232

Lyapustin, A. I., Wang, Y., Laszlo, I., Hilker, T., G.Hall, F., Sellers, P. J., … Korkin, S. V. (2012). Multi-angle implementation of atmospheric correction for MODIS (MAIAC): 3. Atmospheric correction. *Remote Sensing of Environment*, *127*, 385–393. doi:10.1016/j.rse.2012.09.002

Mather, P., & Tso, B. (2016). *Classification methods for remotely sensed data, 2nd ed*. *CRC press*, 159-162.

Mbow, C., Fensholt, R., Nielsen, T. T., & Rasmussen, K. (2014). Advances in monitoring vegetation and land use dynamics in the Sahel. *Geografisk Tidsskrift-Danish Journal of Geography*, (December), 8. doi:10.1080/00167223.2014.88

Minet, J. (2007). Influence de la dispersion du parcellaire sur la gestion du risque climatique au

685 Fakara, Niger. Thesis: *Faculté d'Ingénierie Biologique, Agronomique et Environnementale.*
686 *Université Catholique de Louvain, Louvain-La-Neuve, Belgium.*

687 Nutini, F., Boschetti, M., Brivio, P. a., Bocchi, S., & Antoninetti, M. (2013). Land-use and land-
688 cover change detection in a semi-arid area of Niger using multi-temporal analysis of Landsat
689 images. *International Journal of Remote Sensing*, *34*(January 2015), 4769–4790.
690 doi:10.1080/01431161.2013.781702

691 Olsson, L., Eklundh, L., & Ardö, J. (2005). A recent greening of the Sahel - Trends, patterns and
692 potential causes. *Journal of Arid Environments*, *63*, 556–566.
693 doi:10.1016/j.jaridenv.2005.03.008

694 Osbahr, H. (2001). Livelihood strategies and soil fertility at Fandou Béri, southwestern Niger.
695 Thesis: *Department of Geography. University College London, London.*

696 Rasmussen, K., D'haen, S., Fensholt, R., Fog, B., Horion, S., Nielsen, J. O., … Reenberg, A. (2015).
697 Environmental change in the Sahel: reconciling contrasting evidence and interpretations.
698 *Regional Environmental Change*, 673–680. doi:10.1007/s10113-015-0778-1

699 Rasmussen, L. V., & Reenberg, A. (2012). Land use rationales in desert fringe agriculture. *Applied*
700 *Geography*, *34*, 595–605. doi:10.1016/j.apgeog.2012.03.005

701 Romankiewicz, C., Doevenspeck, M., Brandt, M., & Samimi, C. (2016). Adaptation as by-product:
702 migration and environmental change in Nguith, Senegal. *Die Erde*, *147*(2), 95–108.
703 doi:10.12854/erde-147-7

704 Ross, T. J. (2004). *Fuzzy Logic with Engieering Applications*. *John Wiley & Sons*, 371-387.

705 Sanogo, S., Fink, A. H., Omotosho, J. a., Ba, A., Redl, R., & Ermert, V. (2015). Spatio-temporal

706 characteristics of the recent rainfall recovery in West Africa. *International Journal of*
707 *Climatology*, *35*(15), 4589–4605. doi:10.1002/joc.4309

708 Turner, M. D., & Hiernaux, P. (2015). The effects of management history and landscape position on
709 inter-field variation in soil fertility and millet yields in southwestern Niger. *Agriculture,*
710 *Ecosystems & Environment*, *211*, 73–83. doi:10.1016/j.agee.2015.05.010

711 van Vliet, N., Reenberg, A., Rasmussen, L. V. (2013). Scientific documentation of crop land
712 changes in the Sahel: A half empty box of knowledge to support policy? *Journal of Arid*
713 *Environments*, *95*, 1–13. doi:10.1016/j.jaridenv.2013.03.010

714 Vermote, E. F., El Saleous, N. Z., & Justice, C. O. (2002). Atmospheric correction of MODIS data
715 in the visible to middle infrared: First results. *Remote Sensing of Environment*, *83*(1–2), 97–
716 111. http://doi.org/10.1016/S0034-4257(02)00089-5

717 Vintrou, E., Desbrosse, A., Bégué, A., Traoré, S., Baron, C., & Lo Seen, D. (2012). Crop area
718 mapping in West Africa using landscape stratification of MODIS time series and comparison
719 with existing global land products. *International Journal of Applied Earth Observation and*
720 *Geoinformation*, *14*(1), 83–93. doi:10.1016/j.jag.2011.06.010

721 Penning de Vries, F., & Djiteye, M.A. (1982). La productivité des pâturages sahéliens, une étude
722 des sols, des végétations et de l'exploitation de cette ressource naturelle. *Centre for*
723 *Agricultural Publishing and Documentation*.

724 Wang, F. (1990). Fuzzy Supervised Classification of Remote Sensing Images. *IEEE Transactions*
725 *on Geoscience and Remote Sensing*, *28*(2), 194–201. doi:10.1109/36.46698

726 Wang, X., Piao, S., Xu, X., Ciais, P., Macbean, N., Myneni, R. B., & Li, L. (2015). Has the
727 advancing onset of spring vegetation green-up slowed down or changed abruptly over the last

three decades? *Global Ecology and Biogeography*, *24*(6), 621–631. doi:10.1111/geb.12289

Zhang, Y., Du, Y., Li, X., Fang, S., & Ling, F. (2014). Unsupervised Subpixel Mapping of Remotely Sensed Imagery Based on Fuzzy C-Means Clustering Approach, *11*(5), 1024–1028.

List of Figure Captions

Fig. 1. a) The location of the Fakara region in Niger (red block) within the Sahelian delineation (dashed lines). b) The study area (green block: latitude North 13°23′54″-13° 33′ 57″ , longitude East 2°35′3″-2°49′8″) is located in the Fakara region.

Fig. 2. Flow chart of the methods applied in this study (CF*FF*: the two field types of cropped and fallowed fields). 1) Sampling the two field types; 2) temporal profile extraction; 3) mapping the cropped/fallowed fields and analyzing the relation to NDVI trends.

Fig. 3. a) Land use/cover map showing the location of the 72 transects for the vegetation surveys (Hiernaux et al., 2009). A supervised classification was done using a SPOT 10 m image from September 28, 2004. b) The map insert shows the same SPOT image in a false color composition (patches of bright white and dark red represent cropped and fallowed fields, respectively).

Fig. 4. Scatter plots illustrating the locations of unsupervised FCM generated clusters (red squares). Examples of a) 2 clusters and b) 10 clusters using the inputs of amplitude and the right derivative of the year 2004. A larger number of clusters will facilitate extraction of endmembers for pure cropped and fallowed fields.

Fig. 5. a): Intra-annual NDVI profiles averaged for all cropped/fallowed fields between 2000 and 2014. b): Scatter plot between the annual NDVI average of cropped and fallowed fields. Number (N) of MODIS 8-day composite values (per year) of higher averaged NDVI of fallowed fields than of cropped fields are indicated by the size of the circles.

751 **Fig. 6.** a) Box plots comparing NDVI metrics for cropped and fallowed fields averaged over the period of analysis
752 (2000-2014). b) Plots showing the yearly difference of amplitude (left) and right derivative (right) between cropped and
753 fallowed fields. The standard deviations shown correspond to the variability between samples.

754 **Fig. 7.** Cropped/fallowed field membership map of 2004 using MODIS 250 m resolution seasonal NDVI metrics inputs
755 (amplitude and right derivative).

756 **Fig.8.** Linear regression between FCM membership and fallow percentage (derived from digitalizing SPOT 10 m
757 imageries), plotted for four years (2004, 2008, 2010, and 2012).

758 **Fig. 9.** a) Slope values from linear regression trend analysis of cropped/fallowed field membership maps (2000-2014).
759 Positive slope values mean a direction of change towards more fallows, b) slope values from the linear regression trend
760 analysis of MODIS annual NDVI sum (2000-2014), c) scatter plot showing the relation between slope values of
761 cropped/fallowed field membership and annual NDVI sum, and d) bar plot showing the percentage of cropped and
762 fallowed areas in the Fakara study area. Linear trends are shown for cropped fields, fallowed fields, annual NDVI, and
763 rainfall sum.